TABLE. 1. Model parameters.

Models	r, mm	$\dot{\gamma}$, s^{-1}	D	T_c, K	T_{bl}, K
1	1	10^{-15}	$D_{Al,Opx}$	1050	1321
2	10	10^{-15}	$D_{Al,Opx}$	1050	1321
3	1	10^{-15}	$D_{Fe,Gt}$	1050	1321
4	1	10^{-16}	$D_{Al,Opx}$	1050	1321
5	10	10^{-16}	$D_{Al,Opx}$	1050	1321
6	10	10^{-16}	$D_{Al,Opx}$	1350	1521
7	1	10^{-16}	$D_{Al,Opx}$	1150	1521
8	10	10^{-16}	$D_{Fe,Gt}$	1050	1321

crustal-heat-production dominated. For $\dot{\gamma} = 10^{-15}$ s^{-1}, the observed maximum elevation of mountain belts can be explained as a consequence of disequilibrium phase boundary depth for a wide range of physical parameters, although a comparatively young age for Maxwell Montes (50 m.y.) is implied. For the lesser horizontal strain rate of 10^{-16} s^{-1}, only limited parameter values for thermal models are allowed.

References: [1] Barsukov V. L. et al. (1986) *Proc. LPSC 16th*, in *JGR, 91*, D378. [2] Solomon S. C. et al. (1991) *Science, 252*, 297. [3] Head J. W. et al. (1991) *Science, 252*, 276. [4] Pronin A. A. (1986) *Geotectonics, 20*, 271. [5] Basilevsky A. T. (1986) *Geotectonics, 20*, 282. [6] Grimm R. E. and Phillips R. J. (1990) *GRL, 17*, 1349. [7] Roberts K. M. and Head J. W. (1990) *GRL, 17*, 1341. [8] Bindschadler D. L. and Parmentier E. M. (1990) *JGR, 95*, 21329. [9] Crumpler L. S. et al. (1986) *Geology, 14*, 1031. [10] Surkov Yu. A. et al. (1987) *Proc. LPSC 17th*, in *JGR, 92*, E537. [11] Vorder Bruegge R. W. and Head J. W. (1991) *Geology, 19*, 885. [12] Ahrens T. J. and Schubert G. (1975) *Rev. Geophys. Space Phys., 13*, 383. [13] Ito K. and Kennedy G. C. (1971) *Geophys. Mon., 14*, 303. [14] Smith D. and Barron B. R. (1991) *Am. Mineral., 76*, 1950. [15] Grimm R. E. and Phillips R. J. (1991) *JGR, 96*, 8305. [16] Joesten R. (1991) In *Diffusion, Atomic Ordering and Mass Transport*, 345, Springer-Verlag. [17] Condit R. H. et al. (1985) *Geophys. Mon., 31*, 97.

N93-14351

RESULTS OF A ZONALLY TRUNCATED THREE-DIMENSIONAL MODEL OF THE VENUS MIDDLE ATMOSPHERE.

M. Newman, CIRES, University of Colorado, Boulder CO 80309, USA.

Although the equatorial rotational speed of the solid surface of Venus is only 4 m s^{-1}, the atmospheric rotational speed reaches a maximum of approximately 100 m s^{-1} near the equatorial cloud top level (65 to 70 km). This phenomenon, known as superrotation, is the central dynamical problem of the Venus atmosphere. We report here the results of numerical simulations aimed at clarifying the mechanism for maintaining the equatorial cloud top rotation.

Maintenance of an equatorial rotational speed maximum above the surface requires waves or eddies that systematically transport angular momentum against its zonal mean gradient. The zonally symmetric Hadley circulation is driven thermally and acts to reduce the rotational speed at the equatorial cloud top level; thus wave or eddy transport must counter this tendency as well as friction. Planetary waves arising from horizontal shear instability of the zonal flow (barotropic instability) could maintain the equatorial rotation by transporting angular momentum horizontally from midlatitudes toward the equator. Alternatively, vertically propagating waves could provide the required momentum source. The relative motion between the rotating atmosphere and the pattern of solar heating, which has a maximum where solar radiation is absorbed near the cloud tops, drives diurnal and semidiurnal thermal tides that propagate vertically away from the cloud top level. The effect of this wave propagation is to transport momentum toward the cloud top level at low latitudes and accelerate the mean zonal flow there.

We employ a semispectral primitive equation model with a zonal mean flow and zonal wavenumbers 1 and 2 [1]. These waves correspond to the diurnal and semidiurnal tides, but they can also be excited by barotropic or baroclinic instability. Waves of higher wavenumbers and interactions between the waves are neglected. Symmetry about the equator is assumed, so the model applies to one hemisphere and covers the altitude range 30 to 110 km. Horizontal resolution is 1.5° latitude, and vertical resolution is 1.5 km. Solar and thermal infrared heating, based on Venus observations and calculations drive the model flow [2]. Dissipation is accomplished mainly by Rayleigh friction, chosen to produce strong dissipation above 85 km in order to absorb upward propagating waves and limit extreme flow velocities there, yet to give very weak Rayleigh friction below 70 km; results in the cloud layer do not appear to be sensitive to the Rayleigh friction. The model also has weak vertical diffusion, and very weak horizontal diffusion, which has a smoothing effect on the flow only at the two grid points nearest the pole.

Simulations were carried out with uniform background angular velocity equivalent to an equatorial speed of u_0, where u_0 was varied between 50 and 75 m s^{-1}. Flow with this angular velocity was the initial condition for half of the simulations. The initial condition for the other half was obtained by adding to this background rotation a horizontally uniform, cyclostrophic-balanced component with zero additional zonal velocity at 30 and 110 km and a smooth increase to a maximum addition of 50 m s^{-1} at 65 km on the equator. Model runs were also carried out in which the coefficient of vertical diffusion υ was varied. Cases were run for 350 simulated (Earth) days, by which time a statistically steady state was reached. We present averages for the last 40 days of each run.

In the resulting mean zonal flow, the equilibrated equatorial wind maximum was typically between 90 and 105 m s^{-1}, and a jet developed near 40° latitude. The tides, particularly the semidiurnal tide, acted to balance (upgradient/downgradient) vertical advection by the Hadley cell updraft (below/above) the low-latitude zonal wind maximum. Experiments in which u_0 was vaned indicated that the shape of this vertical jet (i.e., the vertical wind shear) is less sensitive to the background rotation than is the value of the speed maximum. This suggests that any theory that describes the role of the thermal tides in maintaining the equatorial rotational wind structure against vertical advection cannot oversimplify the vertical wind structure. Vertical diffusion acted to counter the tidal acceleration at cloud top, producing a slower zonal wind speed. For example, for two runs employing the sheared 60 m s^{-1} background rotation, reduction of υ from 2.5 to 1.0 m^2 s^{-1} produced an increase of more than 10 m s^{-1} in the equatorial zonal wind maximum. The diurnal tide transported angular momentum horizontally from the region of the midlatitude jet toward lower latitudes, acting to smooth the zonal wind profile between the midlatitude jets and the equator; thus, the jet does not become significantly barotropically unstable.

The tides also acted to weaken the Hadley circulation through both their meridional and upward heat fluxes. At the equator, the vertical convergence of the upward heat flux compensates part of the zonally averaged solar heating in the cloud top region. This effect reduced the mean equatorial cloud-level updraft by half, as compared to zonally symmetric model runs. Thus the tides act to

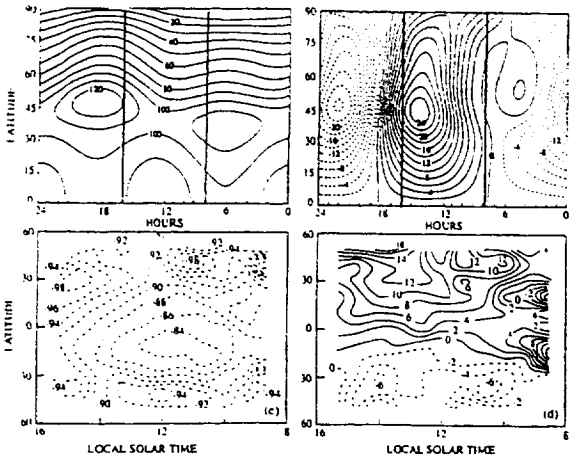

Fig. 1. Comparison of model distributions of cloud top zonal and meridional winds with local time, (a) and (b), with distributions derived from cloud drift measurements, (c) and (d) [3]. The heavy black lines mark the region of UV cloud observations. Model results are averages from the last 40 days of the 350-day simulation with initial sheared angular velocity, for $u_0 = 60\ m\ s^{-1}$ and $\upsilon = 2.5\ m^2\ s^{-1}$.

maintain the mean zonal flow at cloud top level in two ways: directly through tidal fluxes of angular momentum, and indirectly, by reducing the thermal forcing of the Hadley cell.

At the cloud top level, the model zonal wind has a distinct minimum during daytime such that the midlatitude jet is substantially diminished from the zonal mean value. The daytime meridional wind, on the other hand, is strongly poleward and is at a maximum in early afternoon (Fig. 1). This is a robust result that is consistent with both the near absence of midlatitude jets and the strong meridional winds deduced from cloud drifts. Cloud drifts can be measured only during the period from about 0800 to about 1600 hours local time, but they have been used to infer zonally averaged zonal and meridional winds [3]. As shown by the results, this is inappropriate and would lead to spurious estimates.

Also present are nontidal wave components: a wavenumber 2 component with typically a 2.6-day period, and a weaker wavenumber 1 component with the same angular phase speed and 5.2-day period. These are confined mainly to midlatitudes and are due to baroclinic and barotropic instabilities of the zonal mean flow in the lower cloud region. These features may be related to a wavenumber 1 5.2-day spectral feature that has been detected in cloud-level observations. The wavenumber 2 feature became stronger relative to wavenumber 1 as the background rotation was increased between runs, which caused the jet to be centered at slightly lower latitude. This relative wavenumber 2 dominance may also be a consequence of the omission of wave-wave interactions. These waves did not contribute to maintenance of the zonal mean flow near the equator, but in mid to high latitudes they did act to transport momentum from the middle to lower cloud region, and thus possibly contributed to the slight (~5 K) temperature rise in the cloud-top polar region. Although the model did not duplicate the observed cloud top polar warm region, it appears that a higher-latitude jet in the middle cloud region could act to both increase the wavenumber 1 component and duct the waves more toward the pole, inducing warmer temperatures there.

To determine the robustness of these results, further model runs are currently being conducted to more completely explore the parameter space described above. These results also suggest that a Venus GCM will either need sufficient resolution to capture the tides, or else a parameterization scheme that can adequately capture their effects.

References: [1] Holton J. R. and Wehrbein W. (1980) *Pure Appl. Geophys., 284*; Newman M. (1991) thesis, Univ. of Washington; Newman M. and Leovy C. B. (1992) *Science*, submitted. [2] Crisp D. (1983) thesis, Princeton Univ. [3] Limaye S. S. et al. (1988) *Icarus, 90*, 193; Rossow W. B. et al. (1990) *J. Atmos. Sci.*, 2053.

N93-14352

A MODEL FOR THE FORMATION OF THE EXTENDED PARABOLOIDAL HALOS AROUND SOME IMPACT CRATERS ON VENUS.

W. I. Newman[1], E. M. Jones[2], D. B. Campbell[3], and N. J. S. Stacy[3], [1]Departments of Earth and Space Sciences, Astronomy, and Mathematics, University of California, Los Angeles CA 90024–1567, USA, [2]Earth and Environmental Sciences Division, Los Alamos National Laboratory, Los Alamos NM 87545, USA, [3]National Astronomy and Ionosphere Center and Department of Astronomy, Cornell University, Ithaca NY 14853, USA.

Many parabolic-shaped extended impact crater-related features have been found in Magellan synthetic aperture radar and emissivity data covering much of the surface of Venus. They are oriented east-west with the apex to the east and the impact crater located just west of the apex. A model for the formation of the parabolic features is developed based on the injection of small particles into the upper atmosphere at the time of impact, and their subsequent transport to the west by the east-west zonal winds. Fallout times from 50 km in the Venus atmosphere for particles of this size are about two hours, allowing westerly drifts of several hundred kilometers for zonal winds of 50 to 100 m s^{-1}

N93-14353

VENUS: PRELIMINARY GEOLOGIC MAPPING OF NORTHERN ATLA REGIO.

A. M. Nikishin[1] and G. A. Burba[2], [1]Geological Faculty, Moscow State University, 119899, Moscow, Russia, [2]Vernadsky Institute, Russian Academy of Science, 117975, Moscow, Russia.

A preliminary geologic map of C1 sheet 15N197 was compiled according to Magellan data (Fig. 1). Northern Atla Regio is dominantly a volcanic plain with numerous volcanic features: radar-bright and -dark flows and spots, shield volcanos, volcanic domes and hills with varied morphology, and coronalike constructions. Tesserae are the oldest terrains semiflooded by plain materials. There are many lineated terrains on this territory. They are interpreted as old, partly buried ridge belts. Lineated terrains have intermediate age between young plains and old tesserae. Ozza Mons and Sapas Mons are the high shield volcanos.

The prominent structure of northern Atla Regio is Ganis Chasma rift. The rift dissected the volcanic plain and evolved nearly contemporaneously with Ozza Mons shield volcano. Ganis Chasma rift valley is highly fractured and bounded by fault scarps. There are a few relatively young volcanic features in the rift valley. The rift originated due to 5–10% crustal extension and crustal subsidence according to analysis of fracturing and rift valley geometry. Ganis Chasma is characterized by rift shoulder uplifts. Geological structures of Atla Regio and Beta Regio are very similar as assumed earlier [1,2].

References: [1] Nikishin A. M. (1990) *Earth Moon Planets, 50/51*, 101–125. [2] Senske D. A. and Head J. W. (1989) *LPSC XIX*, 986–987.